ASTRONOMY & ASTROPHYSICS
SUPPLEMENT SERIES

Astron. Astrophys. Suppl. Ser. **103,** 273-277 (1994)

Atomic data from the IRON project. II. Effective collision strengths for infrared transitions in carbon-like ions

D.J. Lennon[1] and V.M. Burke[2]

[1] Institut für Astronomie und Astrophysik der Universität München, Scheinerstrasse 1, D-8000 München 80, Germany
[2] SERC Daresbury Laboratory, Warrington WA4 4AD, U.K.

Received May 14; accepted July 6, 1993

Abstract. — We present new calculations of cross-sections for the electron impact excitation of carbon-like ions from N II to S XI, paying particular attention to the infrared transitions between the $2p^2\ ^3P$ $J = 0, 1, 2$ ground state fine-structure levels. We also give rate coefficients, assuming a Maxwellian electron velocity distribution, in the form of effective collision strengths for these transitions up to an electron temperature of 10^5 K. We also give results for transitions involving the other $2p^2$ terms (^1D and ^1S) as well as the $2s2p^3$ (^5S) term. The present results are in excellent agreement with a number of similar calulations available in the literature but are more comprehensive in scope.

Key words: atomic — atomic processes data

1. Introduction

The spectra of many types of gaseous nebulae are dominated by the presence of emission lines, many of them due to forbidden or semi-forbidden transitions of metal ions. In order to model such plasmas, one needs to know the relevant atomic data namely, radiative transition probabilities and electron impact excitation cross-sections. Naturally, lines in the visible part of the spectrum have received the most attention, however following the success of recent satellite-borne ultraviolet (UV) telescopes [such as the International Ultraviolet Explorer], considerable attention has also been given to lines in the near-UV. By contrast, lines lying in the infrared (IR) have been comparatively neglected, to date these observations being limited to balloon or rocket flights and upper atmosphere aeroplane flights. These IR lines, arising mainly from transitions between fine structure levels of ground state terms, are important as they are the dominant cooling mechanism for many astrophysical plasmas. This observational imbalance is to be redressed in the coming years due to the forthcoming launch of IR dedicated satellite-borne telescopes such as the Infrared Space Observatory (ISO) or the Space Infrared Telescope Facility (SIRTF). Thus it is to be expected that many infrared lines previously overlooked will then be detected, indeed estimates have already been made of line strengths for some of these lines, see for example Spinoglio & Malkan (1992) and Voit (1992). Therefore, an international collaborative project has been initiated, called the Iron Project (see Hummer et al. 1993, hereafter Paper I), the first stage of which is to calculate in a systematic way, new electron impact excitation rates with particular emphasis on these IR transitions. [The second, and more ambitious stage, is to calculate new data for ions of iron.]

This paper reports on the results for electron impact excitation rate coefficients (actually effective collision strengths) for transitions between the $2p^2\ ^3P$ J=0,1,2 fine structure levels of ions in the carbon iso-electronic sequence (ions with six electrons) from N II (nuclear charge $z = 7$) to S XI ($z = 16$). A complete list of the wavelengths for these IR transitions is given in Table 1. As a corollary to this work, we also give results for transitions involving the other $2p^2$ terms (^1D and ^1S) plus the $2s2p^3\ ^5S$ term since a number of these transitions are important diagnostics for astrophysical plasmas in the visible and ultraviolet spectral regions. Previous work on the carbon sequence ions is extensive, Hebb & Menzel (1940) performed the first calculation for O III while Blaha (1969) and Saraph et al. (1969) computed early estimates of cross-sections for iso-electronic sequences, including the C-sequence. More recent close-coupling calculations for ions of this sequence, in which the effect of resonances are included, have been performed mainly by two groups at University College London (see Eissner & Seaton (1972,1974), Jackson (1973), Saraph & Seaton (1974), Giles (1979) and

Giles et al. (1979)) and the Queen's University of Belfast (see Baluja, Burke & Kingston (1980), Aggarwal et al. (1982,1983a,1983b, 1984) and Johnson et al. (1987). However, while this work provides excellent data for a number of ions, notably C I, O III, Ne V, Mg VII and Si IX, other ions have been comparatively neglected.

Table 1. Wavelengths (in μm) of the infrared transitions for carbon sequence ions taken from the compilations of Wiese et al. (1966,1969) except that the values for S XI are estimated from the energy levels given by Martin et al. (1990)

Ion	$^3P_0$-$^3P_1$	$^3P_0$-$^3P_2$	$^3P_1$-$^3P_2$
N II	203.6	76.14	121.6
O III	88.16	32.59	51.6
F IV	44.39	16.30	25.75
Ne V	24.15	8.99	14.32
Na VI	14.32	5.3807	8.6183
Mg VII	8.8707	3.4016	5.5173
Al VIII	5.7456	2.2516	3.7027
Si IX	3.8600	1.5476	2.5833
P X	2.9491	1.1652	1.9263
S XI	1.9201	0.8072	1.3927

2. New calculations

We have used the revised versions of the RMATRX codes as described by Berrington et al. (1987), the target wavefunctions being generated by the general configuration interaction code CIV3 (Hibbert 1975). The same procedure was followed here as was used by Burke et al. (1989) for O III and Lennon & Burke (1991) for Ne V where further details may be found. [In fact the results given here for these two ions are a repeat of these previous calculations, though using a new asymptotic code, which we give for completeness.] All twelve target states belonging to the $2s^22p^2$, $2s2p^3$ and $2p^4$ configurations were included in the target, and for the scattering calculation the diagonal elements of the Hamiltonian matrix were adjusted so as to obtain excitation thresholds in agreement with experiment. All partial waves with $L \leq 4$ were included which should be sufficient to ensure convergence for the transitions of interest, except perhaps for the ^{1}D-^{1}S transition where there is a small contribution from higher partial waves, see the discussion of Eissner & Seaton (1974) or Aggarwal (1984) for example. We employed an energy mesh similar to that used by Burke et al. (1989) and fine-structure collision strengths were computed using STGFJ. A more complete discussion of the methods used may be found in Paper I. Assuming a Maxwellian distribution of electron velocities, these data were then used to calculate effective collision strengths according to the linear interpolation scheme described by Burgess & Tully (1992). Note that formally in calculating an excitation rate one must extrapolate the calculated cross-section to infinity. In the present work however, for all transitions under consideration, collision strengths were calculated to sufficiently high energy to ensure that the extrapolated contribution from higher energies to the numerical integration was negligible, even at the highest electron temperature considered. In all cases this contribution was less than 1% of the final result.

3. Results

The effective collision strengths are tabulated in Tables 2 through 11 and for illustrative purposes we show the behaviour of the results for the $^3P_0$-$^3P_1$ transition as a function of electron temperature in Figs. 1 and 2. In these tables we have not explicitly given values for the fine structure transitions between the ^3P ground state and the ^1D, ^1S and ^5S states as these may be derived from the total effective collision strength using the formula,

$$\Upsilon(^3\mathrm{P}_{J'} - {}^S\mathrm{L}_J) = \frac{2J'+1}{9}\Upsilon(^3\mathrm{P} - {}^S\mathrm{L}_J) \qquad (1)$$

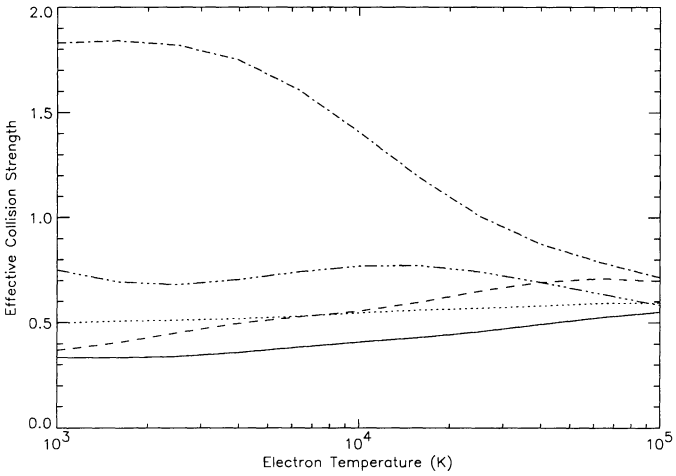

Fig. 1. Effective collision strengths for the $^3P_0$-$^3P_1$ transition for N II (solid line), O III (dotted line), F IV (dashed line), Ne V (dash-dotted line) and Na VI (dash-dot-dot-dotted line)

where J' is the J-value of the ^{3}P level of interest and $^S\mathrm{L}_J$ is one of ^{1}D, ^{1}S or ^{5}S. Note that the effective collision strength ($\Upsilon(i,j)$) for a transition from level i to level j is related to the excitation rate coefficient ($\alpha(i,j)$) through,

$$\alpha(i,j) = \frac{8.63\ 10^{-6}}{g_i T^{1/2}} \exp\left(-\frac{E_{ij}}{kT}\right) \Upsilon(i,j)\ \mathrm{cm^3 s^{-1}} \qquad (2)$$

where E_{ij} is the energy difference between levels i and j, g_i is the statistical weight of level i, T is the electron temperature and k is Boltzmann's constant. The de-excitation

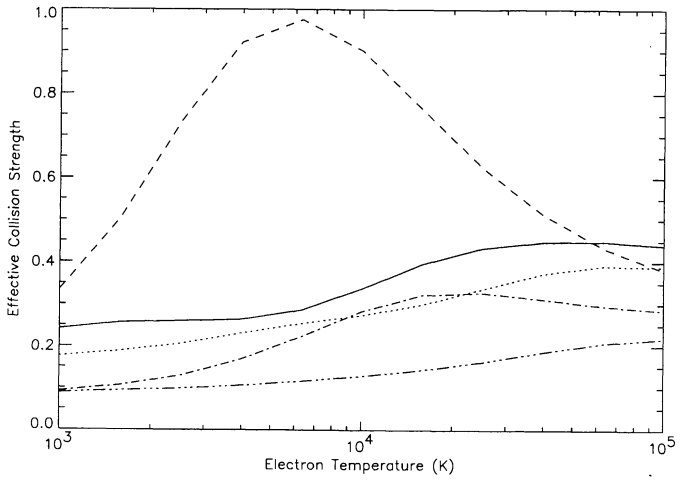

Fig. 2. Effective collision strengths for the $^3P_0$-$^3P_1$ transition for Mg VII (solid line), Al VIII (dotted line), Si IX (dashed line), P X (dash-dotted line) and S XI (dash-dot-dot-dotted line)

rate coefficient is then given by,

$$\alpha(j,i) = \frac{8.63\ 10^{-6}}{g_j T^{1/2}} \Upsilon(i,j)\ \mathrm{cm^3 s^{-1}}. \qquad (3)$$

The enhancement of the effective collision strengths at low temperatures for Ne V and Si IX is due to the influence of resonances, as discussed by Lennon & Burke (1991), Aggarwal (1983a) and Aggarwal (1983b). The accuracy of the results for these two ions depends crucially on the reliability of the calculated positions of the autoionizing states which give rise to these resonances. As has already been pointed out in the references above, this is difficult to quantify as there are as yet no experimental energy levels available for these states. It would be useful however if better theoretical energies were to be computed for these levels to help resolve this question. Nevertheless, we note that the present results agree very well those of Aggarwal (1983a, 1983b) and further, that the results for O III and Mg VII are also in excellent agreement with similar calculations performed by Aggarwal et al. (1982) and Aggarwal (1984). Comparable calculations for the infared transitions of the remaining ions considered here have not yet been performed, however we have no reason to suppose that these results are any less reliable.

Acknowledgements. We would like to thank Keith Butler for help and advice on using the atomic physics codes, and to David Hummer and Keith Berrington for helpful comments on the original draft of this paper. DJL is grateful for support from the Bundesminister für Forschung und Technologie under grant 010 R 90080.

References

Aggarwal K.M. 1983a, J. Phys. B 16, 2405
Aggarwal K.M. 1983b, J. Phys. B 16, L59
Aggarwal K.M. 1984, Sol. Phys. 94, 75
Aggarwal K.M., Baluja K.L., Tully J.A. 1982, MNRAS 201, 923
Baluja K.L., Burke P.G., Kingston A.E. 1980, J. Phys. B 13, 4675
Berrington K.A., Burke P.G., Butler K., Seaton M.J., Storey P.J., Taylor K.T., Yu Yan 1987, J. Phys. B 20, 6379
Blaha M. 1969, A&A 1, 42
Burgess A., Tully J.A. 1992, A&A 254, 436
Burke V.M., Lennon D.J., Seaton M.J. 1989, MNRAS 236, 353
Eissner W., Seaton M.J. 1972, J. Phys. B 5, 2187
Eissner W., Seaton M.J. 1974, J. Phys. B 7, 2533
Giles K. 1979, MNRAS 187, L49
Giles K., Jackson A.R.G., Pradhan A.K. 1979, J. Phys. B 12, 3415
Hebb M.H., Menzel D.H. 1940, ApJ 92, 408
Hibbert A. 1975, Comp. Phys. Comm. 9, 141
Hummer D.G., Berrington K.A., Eissner W., Pradhan A.K., Saraph H.E., Tully J.A. 1993, A&A, submitted (Paper I)
Jackson A.R.G. 1973, MNRAS 165, 53
Johnson C.T., Burke P.G., Kingston A.E. 1987, J. Phys. B 20, 2553
Lennon D.J., Burke V.M. 1991, MNRAS 251, 628
Martin W.C., Zalubas R., Musgrove A. 1990, J. Phys. Chem. Ref. Data 19, 821
Saraph H.E., Seaton M.J. 1974, J. Phys. B 7, L36
Saraph H.E., Seaton M.J., Shemming J. 1969, Phil. Trans. R. Soc. London Ser. A 264, 77
Spinoglio L., Malkan M.A. 1992, ApJ 399, 504
Voit G.M. 1992, ApJ 399, 495
Wiese W.L, Smith M.W., Glennon B.M. 1966, Atomic Transition Probabilities, Vol. I: Hydrogen Through Neon, NSRDS-NBS 4 Vol. I., US Gov. Printing Office
Wiese W.L, Smith M.W., Glennon B.M. 1969, Atomic Transition Probabilities, Vol. II: Sodium Through Argon, NSRDS-NBS 4 Vol. II., US Gov. Printing Office

1994A&AS..103..273L

Table 2. Effective collision strengths for N II

	Transition						
log T(K)	$^3P_0$-$^3P_1$	$^3P_0$-$^3P_2$	$^3P_1$-$^3P_2$	^3P-$^1D_2$	^3P-$^1S_0$	^3P-$^5S_2$	$^1D_2$-$^1S_0$
3.0	0.3336	0.2142	0.8978	2.4841	0.2813	1.1971	1.1640
3.2	0.3333	0.2194	0.9092	2.4963	0.2821	1.1958	1.1260
3.4	0.3394	0.2256	0.9307	2.5163	0.2833	1.1940	1.0710
3.6	0.3581	0.2351	0.9753	2.5469	0.2853	1.1913	0.9998
3.8	0.3837	0.2499	1.0410	2.5884	0.2884	1.1883	0.9176
4.0	0.4076	0.2720	1.1200	2.6409	0.2931	1.1903	0.8338
4.2	0.4293	0.3012	1.2130	2.7000	0.2999	1.2050	0.7605
4.4	0.4566	0.3316	1.3160	2.7663	0.3099	1.2248	0.7097
4.6	0.4910	0.3524	1.4050	2.8444	0.3240	1.2299	0.6825
4.8	0.5238	0.3572	1.4580	2.9235	0.3396	1.2071	0.6686
5.0	0.5499	0.3494	1.4730	2.9668	0.3524	1.1545	0.6571

Table 3. Effective collision strengths for O III

	Transition						
log T(K)	$^3P_0$-$^3P_1$	$^3P_0$-$^3P_2$	$^3P_1$-$^3P_2$	^3P-$^1D_2$	^3P-$^1S_0$	^3P-$^5S_2$	$^1D_2$-$^1S_0$
3.0	0.4975	0.2455	1.1730	2.2233	0.2754	0.9760	0.4241
3.2	0.5066	0.2493	1.1930	2.1888	0.2738	0.9673	0.4268
3.4	0.5115	0.2509	1.2030	2.1416	0.2713	0.9712	0.4357
3.6	0.5180	0.2541	1.2180	2.1117	0.2693	1.0224	0.4652
3.8	0.5296	0.2609	1.2480	2.1578	0.2747	1.1196	0.5232
4.0	0.5454	0.2713	1.2910	2.2892	0.2925	1.2074	0.5815
4.2	0.5590	0.2832	1.3350	2.4497	0.3174	1.2574	0.6100
4.4	0.5678	0.2955	1.3730	2.5851	0.3405	1.2720	0.6090
4.6	0.5788	0.3101	1.4190	2.6730	0.3563	1.2451	0.5971
4.8	0.5918	0.3254	1.4680	2.7019	0.3621	1.1704	0.5865
5.0	0.5938	0.3314	1.4820	2.6594	0.3571	1.0600	0.5725

Table 4. Effective collision strengths for F IV

	Transition						
log T(K)	$^3P_0$-$^3P_1$	$^3P_0$-$^3P_2$	$^3P_1$-$^3P_2$	^3P-$^1D_2$	^3P-$^1S_0$	^3P-$^5S_2$	$^1D_2$-$^1S_0$
3.0	0.3687	0.1413	0.7778	2.5218	0.2907	0.9493	0.2977
3.2	0.4047	0.1596	0.8638	2.5073	0.2956	0.9583	0.3024
3.4	0.4518	0.1895	0.9901	2.5559	0.3000	0.9315	0.3054
3.6	0.4959	0.2277	1.1310	2.6392	0.3078	0.9193	0.3081
3.8	0.5268	0.2630	1.2490	2.7069	0.3189	0.9430	0.3128
4.0	0.5536	0.2922	1.3490	2.7338	0.3296	0.9786	0.3245
4.2	0.5962	0.3251	1.4760	2.7201	0.3357	1.0135	0.3461
4.4	0.6494	0.3677	1.6380	2.6763	0.3357	1.0440	0.3782
4.6	0.6920	0.4128	1.7920	2.6139	0.3312	1.0517	0.4240
4.8	0.7108	0.4455	1.8860	2.5344	0.3228	1.0136	0.4745
5.0	0.6977	0.4508	1.8790	2.4159	0.3094	0.9277	0.5050

Table 5. Effective collision strengths for Ne V

	Transition						
log T(K)	$^3P_0$-$^3P_1$	$^3P_0$-$^3P_2$	$^3P_1$-$^3P_2$	^3P-$^1D_2$	^3P-$^1S_0$	^3P-$^5S_2$	$^1D_2$-$^1S_0$
3.0	1.8300	3.2280	9.5510	1.7871	0.3155	0.2806	0.5289
3.2	1.8400	3.1950	9.4880	2.0001	0.2967	0.3435	0.6767
3.4	1.8200	2.9820	8.9840	2.1171	0.2765	0.5658	0.7354
3.6	1.7500	2.6430	8.1330	2.1442	0.2597	0.9418	0.7009
3.8	1.6080	2.2350	7.0380	2.1153	0.2491	1.2803	0.6251
4.0	1.4080	1.8100	5.8320	2.0863	0.2457	1.4258	0.5774
4.2	1.1920	1.4160	4.6750	2.1118	0.2486	1.3933	0.6103
4.4	1.0060	1.0960	3.7220	2.1761	0.2538	1.2871	0.6878
4.6	0.8752	0.8709	3.0490	2.2105	0.2564	1.1764	0.7299
4.8	0.7879	0.7205	2.5970	2.1748	0.2538	1.0638	0.7148
5.0	0.7157	0.6098	2.2540	2.0668	0.2452	0.9343	0.6621

Table 6. Effective collision strengths for Na VI

	Transition						
log T(K)	$^3P_0$-$^3P_1$	$^3P_0$-$^3P_2$	$^3P_1$-$^3P_2$	^3P-$^1D_2$	^3P-$^1S_0$	^3P-$^5S_2$	$^1D_2$-$^1S_0$
3.0	0.7506	0.5294	2.1300	1.7356	0.1769	0.2976	0.0978
3.2	0.6948	0.4828	1.9550	1.7075	0.1757	0.2943	0.0995
3.4	0.6803	0.4702	1.9080	1.6532	0.1748	0.2925	0.1021
3.6	0.7052	0.4899	1.9840	1.5870	0.1738	0.3009	0.1053
3.8	0.7422	0.5140	2.0840	1.5182	0.1727	0.3483	0.1094
4.0	0.7697	0.5214	2.1330	1.4505	0.1718	0.4538	0.1157
4.2	0.7725	0.5082	2.1020	1.3947	0.1720	0.5838	0.1276
4.4	0.7428	0.4807	1.9950	1.3602	0.1746	0.6886	0.1498
4.6	0.6922	0.4504	1.8530	1.3466	0.1789	0.7449	0.1887
4.8	0.6372	0.4246	1.7180	1.3417	0.1823	0.7461	0.2410
5.0	0.5825	0.3995	1.5890	1.3232	0.1815	0.6954	0.2876

Table 7. Effective collision strengths for Mg VII

	Transition						
log T(K)	$^3P_0$-$^3P_1$	$^3P_0$-$^3P_2$	$^3P_1$-$^3P_2$	^3P-$^1D_2$	^3P-$^1S_0$	^3P-$^5S_2$	$^1D_2$-$^1S_0$
3.0	0.2414	0.1787	0.7038	0.7362	0.1998	0.8217	0.3201
3.2	0.2565	0.1795	0.7245	0.7344	0.2150	0.9880	0.4201
3.4	0.2597	0.1690	0.7049	0.7496	0.2225	1.0484	0.5110
3.6	0.2633	0.1688	0.7086	0.7776	0.2162	0.9827	0.5417
3.8	0.2858	0.2115	0.8298	0.8135	0.2006	0.8426	0.5099
4.0	0.3366	0.3005	1.0790	0.8567	0.1849	0.6970	0.4461
4.2	0.3952	0.3879	1.3240	0.9105	0.1753	0.5973	0.3902
4.4	0.4333	0.4303	1.4460	0.9739	0.1705	0.5560	0.3735
4.6	0.4476	0.4307	1.4560	1.0330	0.1670	0.5506	0.3859
4.8	0.4488	0.4132	1.4200	1.0670	0.1627	0.5474	0.3965
5.0	0.4396	0.3873	1.3570	1.0651	0.1564	0.5211	0.3901

1994A&AS..103..273L

Table 8. Effective collision strengths for Al VIII

	Transition						
log T(K)	$^3P_0$-$^3P_1$	$^3P_0$-$^3P_2$	$^3P_1$-$^3P_2$	^3P-$^1D_2$	^3P-$^1S_0$	^3P-$^5S_2$	$^1D_2$-$^1S_0$
3.0	0.1756	0.0714	0.3787	2.3957	0.0921	0.1552	0.9172
3.2	0.1880	0.0780	0.4088	2.3562	0.1002	0.1540	1.0600
3.4	0.2053	0.0869	0.4503	2.2370	0.1043	0.1565	1.1130
3.6	0.2303	0.0997	0.5102	2.0213	0.1059	0.1773	1.0610
3.8	0.2538	0.1130	0.5693	1.7733	0.1064	0.2401	0.9461
4.0	0.2735	0.1255	0.6220	1.5566	0.1067	0.3367	0.8047
4.2	0.2994	0.1462	0.6995	1.3854	0.1066	0.4258	0.6548
4.4	0.3365	0.1839	0.8269	1.2519	0.1070	0.4800	0.5142
4.6	0.3726	0.2280	0.9648	1.1437	0.1083	0.5025	0.4018
4.8	0.3912	0.2585	1.0500	1.0532	0.1098	0.5007	0.3301
5.0	0.3887	0.2679	1.0620	0.9751	0.1100	0.4734	0.2923

Table 9. Effective collision strengths for Si IX

	Transition						
log T(K)	$^3P_0$-$^3P_1$	$^3P_0$-$^3P_2$	$^3P_1$-$^3P_2$	^3P-$^1D_2$	^3P-$^1S_0$	^3P-$^5S_2$	$^1D_2$-$^1S_0$
3.0	0.3346	0.2480	0.9757	0.5939	0.0818	0.1721	0.0634
3.2	0.5034	0.3556	1.4240	0.5944	0.0811	0.1709	0.0631
3.4	0.7335	0.5145	2.0500	0.6156	0.0807	0.1705	0.0631
3.6	0.9209	0.6529	2.5660	0.6523	0.0803	0.1683	0.0637
3.8	0.9754	0.6974	2.7120	0.6828	0.0802	0.1656	0.0663
4.0	0.9016	0.6452	2.4980	0.6921	0.0809	0.1731	0.0721
4.2	0.7636	0.5441	2.1070	0.6858	0.0845	0.2014	0.0795
4.4	0.6243	0.4440	1.7180	0.6771	0.0910	0.2473	0.0890
4.6	0.5127	0.3663	1.4100	0.6736	0.0971	0.2955	0.1063
4.8	0.4334	0.3118	1.1920	0.6740	0.1006	0.3288	0.1312
5.0	0.3805	0.2748	1.0460	0.6701	0.1008	0.3350	0.1548

Table 10. Effective collision strengths for P X

	Transition						
log T(K)	$^3P_0$-$^3P_1$	$^3P_0$-$^3P_2$	$^3P_1$-$^3P_2$	^3P-$^1D_2$	^3P-$^1S_0$	^3P-$^5S_2$	$^1D_2$-$^1S_0$
3.0	0.0918	0.0398	0.2042	0.4961	0.0721	0.1942	0.0864
3.2	0.1058	0.0546	0.2551	0.5023	0.0716	0.2163	0.0895
3.4	0.1287	0.0959	0.3764	0.5130	0.0717	0.2204	0.0894
3.6	0.1675	0.1708	0.5907	0.5289	0.0743	0.2252	0.0906
3.8	0.2226	0.2551	0.8348	0.5577	0.0808	0.2472	0.0991
4.0	0.2828	0.3163	1.0190	0.5950	0.0883	0.2829	0.1131
4.2	0.3219	0.3339	1.0820	0.6221	0.0922	0.3177	0.1294
4.4	0.3273	0.3125	1.0310	0.6336	0.0919	0.3400	0.1534
4.6	0.3121	0.2762	0.9347	0.6354	0.0897	0.3489	0.1814
4.8	0.2962	0.2470	0.8576	0.6278	0.0872	0.3460	0.1998
5.0	0.2855	0.2290	0.8114	0.6097	0.0848	0.3296	0.2056

Table 11. Effective collision strengths for S XI

	Transition						
log T(K)	$^3P_0$-$^3P_1$	$^3P_0$-$^3P_2$	$^3P_1$-$^3P_2$	^3P-$^1D_2$	^3P-$^1S_0$	^3P-$^5S_2$	$^1D_2$-$^1S_0$
3.0	0.0879	0.0455	0.2112	0.4282	0.0548	0.1721	0.1106
3.2	0.0936	0.0484	0.2248	0.4430	0.0545	0.3864	0.1185
3.4	0.0980	0.0501	0.2342	0.4536	0.0554	0.6004	0.1592
3.6	0.1052	0.0519	0.2472	0.4744	0.0586	0.6931	0.2723
3.8	0.1157	0.0544	0.2662	0.5195	0.0628	0.6578	0.4289
4.0	0.1279	0.0591	0.2917	0.5740	0.0651	0.5585	0.5409
4.2	0.1429	0.0691	0.3319	0.6122	0.0647	0.4562	0.5597
4.4	0.1621	0.0864	0.3929	0.6210	0.0628	0.3826	0.5010
4.6	0.1858	0.1110	0.4746	0.6042	0.0609	0.3407	0.4093
4.8	0.2072	0.1354	0.5525	0.5748	0.0599	0.3181	0.3238
5.0	0.2180	0.1500	0.5957	0.5423	0.0594	0.2982	0.2620